

Evaluation using an LES Database of Constitutive Relations for Fluid-Particle Velocity Correlations in Fully-Developed Gas-Particle Channel Flows

Kulwinder Singh¹, Kyle D. Squires¹ and Olivier Simonin²

1: Department of Mechanical and Aerospace Engineering, Arizona State University, Tempe, Arizona 85287, USA,
kulwinder.singh@asu.edu, squires@asu.edu

2: Institut de Mécanique des Fluides; UMR 5502 CNRS/INPT/UPS Allée du Professeur Camille Soula, 31400 Toulouse,
France, simonin@imft.fr

Abstract Models of the fluid-particle velocity correlation are evaluated in fully-developed particle-laden turbulent channel flow. The database for the model evaluations is generated using Large-Eddy Simulation (LES) of the carrier phase flow combined with Discrete Particle Simulation (DPS) for the dispersed phase. The current focus is on gas-solid flows for which the particle equation of motion includes the contribution from the drag force and the influence of particle momentum exchange on properties of the carrier phase is neglected. Three particle Stokes numbers are considered that provide a wide range in the particle response to the turbulent fluid motions. For each Stokes number, simulations are performed with and then without the influence of inter-particle collisions. Binary particle-particle collisions are considered that are assumed perfectly elastic. Models for the fluid-particle correlation are developed from the Lagrangian stochastic equations of Simonin *et al.* (1993) and Minier and Peirano (2001). The model evaluations are performed using an *in medio* approach in which some terms are supplied from the LES/DPS database with closures applied for the remaining terms. A coupled system of equations is then solved for the fluid-particle correlation tensor. The *in medio* evaluations show that the fluid-particle correlations predicted using the approach proposed by Simonin *et al.* (1993) are reasonably accurate for the parameter ranges considered. While the stochastic equation of Minier and Peirano (2001) also leads to reasonably accurate predictions of the fluid-particle correlation in flows without inter-particle collisions, the model predictions are substantially less accurate in flows that include particle-particle collisions.

1 Introduction

Gas-solid turbulent flows occur in a wide variety of applications of both scientific and technological interest. Simulation strategies for predicting these flows represent an important element in the analysis and design of the devices in which these flows occur. For practical applications, simulation strategies that require substantial empirical input will continue to form the basis for the vast majority of engineering predictions. Thus, the development and assessment of statistical models of many of the effects governing gas-solid flows comprises an important area of research.

The focus of the current effort is on modeling two-phase flows in which the dispersed phase is comprised of a dilute concentration of solid particles suspended within a turbulent gas-phase carrier flow. Dilute gas-solid turbulent flows are not easily predicted because of the complex interactions that occur between the particles and turbulence. Because of the large difference in density between the particles and fluid, the motion of particles that are small compared to the lengthscales of the gas-phase turbulent motion may still exhibit significant slip relative to the carrier-phase velocity. The particle will be responsive to only a fraction of turbulent motions in the gas, with the response of a small particle in a gas-solid flow being dictated by its response time.

Regardless the particular choice of numerical simulation technique – Lagrangian particle tracking methods or Eulerian solution of moment equations – accurate prescription of the correlation between the velocities of the particle and surrounding fluid is central to accurate prediction. This complicates measurements of turbulent two-phase flows because of the difficulty in acquiring quantities in the reference frame attached to a particle. The importance of fluid-particle correlated motion and the need

to model fluid turbulence along particle trajectories supply strong motivation for use of techniques such as Direct Numerical Simulation (DNS) and Large-Eddy Simulation (LES) to model the carrier-phase flow. These techniques offer useful tools for prediction of the interactions governing the carrier phase and in turn a detailed database to study particle-turbulence interactions, albeit over limited ranges and with some empiricism (e.g., low Reynolds numbers and with models of particle dynamics). The methods have proven very useful for fundamental studies of particle-turbulence and particle-particle interactions in gas-solid flows (e.g., see Sommerfeld 2000). The databases generated from such simulations are increasingly used to assess closure models for practical applications.

Using either measurements from experiments or the results from DNS or LES, the evaluation of engineering turbulence models is nearly always performed in an *a priori* or *a posteriori* fashion. *A priori* tests are usually performed using a DNS or LES database – simulation results are used to evaluate a given model relation describing a particular quantity, e.g., the fluid-particle covariance as possibly modeled in terms of the fluid kinetic energy and other variables. In *a posteriori* tests, a set of model equations is solved in order to assess the overall accuracy of predictions of both the continuous and dispersed phases.

While such evaluations have been and will continue to be useful, it is important to recognize the limitations inherent to each approach. *A priori* tests do not account for the fact that a modeled variable such as the fluid-particle covariance is obtained from solution of a differential equation and simple algebraic evaluation of a model relation offers no insight into the mathematical properties of the model. *A posteriori* tests require a full solution of the model equations and introduce ambiguity into the identification of the cause for discrepancies between a model prediction and experimental measurement or DNS/LES result.

In this contribution, an approach that is intermediate – *in medio* – between *a priori* and *a posteriori* tests solves the model equation for a given quantity in which some of the terms are evaluated using results from a DNS or LES database. The procedure offers the advantage over *a priori* tests of incorporating the influence of the differential equation governing the modeled variable and over *a posteriori* tests of isolating the effect of a given closure on prediction of the variable of interest. Similar approaches to evaluating closure models have been applied in single-phase turbulence by Hanjalić (1994) and Parneix *et al.* (1998).

Reported in this manuscript are *in medio* tests of models for fluid-particle correlated motion in particle-laden turbulent channel flow. The primary modeling approach evaluated is that outlined in Simonin *et al.* (1993) in which the equation governing the fluid-particle velocity covariance is developed from a stochastic Lagrangian description of the fluid turbulent velocity along particle paths using a Langevin-type closure model. Predictions of the fluid-particle covariance obtained using the Lagrangian stochastic model of Minier and Peirano (2001) are also assessed. The database used for the evaluations is supplied from LES of turbulent channel flow for the continuous phase and Discrete Particle Simulation (DPS) for the dispersed phase. The influence of the particle response time and effect of inter-particle collisions are investigated. Summarized in the next section is the modeling approach and the use of two Langevin-type equations for deriving transport equations governing the fluid-particle covariance. The procedure for performance of the *in medio* tests are subsequently described followed by a presentation of the results and a summary of the work.

2 Model Development

The joint fluid-particle probability density function $f_{fp}(\mathbf{c}_p, \mathbf{c}_f; \mathbf{x}, t)$ is defined as the probable number of particles in volume $[\mathbf{x}, \mathbf{x} + \delta\mathbf{x}]$ at time t , with velocity \mathbf{v}_p in $[\mathbf{c}_p, \mathbf{c}_p + \delta\mathbf{c}_p]$ and with undisturbed fluid velocity $\tilde{\mathbf{u}}_f$ at the particle position in $[\mathbf{c}_f, \mathbf{c}_f + \delta\mathbf{c}_f]$. The transport equation for f_{fp} can be

derived in a general manner as,

$$\frac{\partial f_{fp}}{\partial t} + \frac{\partial}{\partial x_k} [c_{p,k} f_{fp}] = -\frac{\partial}{\partial c_{p,k}} \left[\left\langle \frac{d v_{p,k}}{dt} \middle| \mathbf{c}_p, \mathbf{c}_f \right\rangle f_{fp} \right] - \frac{\partial}{\partial c_{f,k}} \left[\left\langle \frac{d \tilde{u}_{f,k}}{dt} \middle| \mathbf{c}_p, \mathbf{c}_f \right\rangle f_{fp} \right] + \left(\frac{\partial f_{fp}}{\partial t} \right)_{coll} \quad (1)$$

(e.g., see Simonin 2000). The first term on the right-hand side of (1) represents the effects of external forces on the particle path, the second term represents the effects of fluid turbulence following the particle, and the last term accounts for the modification of the joint fluid-particle pdf by inter-particle collisions. The specific forms for the first two terms on the right-hand side of (1) are considered next.

2.1 Particle equation of motion

The focus of the current simulations and models is on dilute gas-solid flows for which the mass loading ratio is negligible. The particle diameter d_p is small compared to the smallest turbulent lengthscales of the undisturbed fluid flow. The particle density is much larger than that of fluid phase ($\rho_f \ll \rho_p$) where ρ_f is the fluid density and the ρ_p is the particle density. Consequently, the particle response time is large compared to the Kolmogorov timescale of the undisturbed flow. For the dilute regimes under consideration the volume force induced by the surrounding fluid flow on the particles reduces to the drag. The equation of motion for a single particle is written as,

$$\frac{d v_{p,i}}{dt} = -\frac{3}{4} \frac{\rho_f}{\rho_p} \frac{C_D}{d_p} |\mathbf{v}_r| v_{r,i}, \quad (2)$$

where $v_{p,i}$ is the i^{th} component of the particle velocity and $v_{r,i}$ is the particle relative velocity,

$$v_{r,i} = v_{p,i} - \tilde{u}_{f,i}, \quad C_D = \frac{24}{Re_p} (1 + 0.15 Re_p^{0.687}), \quad Re_p = \frac{|\mathbf{v}_r| d_p}{\nu_f}. \quad (3)$$

As shown in (3), the correlation for the drag coefficient from Schiller and Nauman (1935) is introduced to extend the Reynolds number range of the drag force. From (2), the particle relaxation timescale is defined as,

$$\tau_p = \frac{4}{3} \frac{\rho_p}{\rho_f} \frac{d_p}{C_D} \frac{1}{|\mathbf{v}_p - \tilde{\mathbf{u}}_f|}. \quad (4)$$

2.2 Modeling of the fluid turbulence following the particle

Specific forms for the fluid-particle covariance can be constructed from (1) by introducing a model for the acceleration of the fluid following the particle, i.e., the second term on the right-hand side of (1). In this study, the bulk of evaluations are based on use of the Langevin equation proposed by Simonin *et al.* (1993) for the undisturbed fluid velocity measured along the particle trajectory:

$$d\tilde{u}_{f,i} = -\frac{1}{\rho_f} \frac{\partial P_f}{\partial x_i} \delta t + [v_{p,j} - \tilde{u}_{f,j}] \frac{\partial U_{f,i}}{\partial x_j} \delta t + G_{fp,ij} (\tilde{u}_{f,j} - U_{f,j}) \delta t + K_{fp} \delta W_{fp,i} \quad (5)$$

where P_f is the mean fluid pressure, $U_{f,i}$ is the mean fluid velocity, $\delta W_{fp,i}$ represents a Weiner process and K_{fp} is a model coefficient depending on turbulence statistics and can be linked to the fluid dissipation rate ε_f and the Kolmogorov constant, $C_0 = 2.1$. The second-order tensor $G_{fp,ij}$ has dimensions of frequency and models the fluid statistics viewed by the particles. It can be shown by comparison to the Navier-Stokes equation governing the undisturbed fluid motion that the terms containing $G_{fp,ij}$ and K_{fp} jointly model the turbulent pressure gradient, turbulent viscous forces, and

crossing trajectory effects. The success/accuracy of the Langevin equation (5) in modeling these statistical properties is dependent on the particular form of $G_{fp,ij}$. In this work a simple spherical form is used,

$$G_{fp,ij} = -\frac{1}{\tau_{fp}^t} \delta_{ij}, \quad (6)$$

where τ_{fp}^t is the eddy-particle interaction timescale and modeled in terms of the fluid turbulence kinetic energy q_f^2 and dissipation rate ε_f ,

$$\tau_{fp}^t = \frac{1}{\beta_1} \frac{q_f^2}{\varepsilon_f}, \quad \beta_1 = \frac{1}{2} + \frac{3}{4} C_0. \quad (7)$$

In addition to (5), models for the fluid-particle covariance developed from a second Lagrangian stochastic equation are also evaluated. The particular form is that from Minier and Peirano (2001),

$$d\tilde{u}_{f,i} = -\frac{1}{\rho_f} \frac{\partial P_f}{\partial x_i} \delta t + [V_{p,j} - \langle \tilde{u}_{f,j} \rangle_p] \frac{\partial U_{f,i}}{\partial x_j} \delta t + G_{fp,ij}^* (\tilde{u}_{f,j} - U_{f,j}) \delta t + K_{fp}^* \delta W_{fp,i}, \quad (8)$$

where $V_{p,j}$ is the j^{th} component of the mean particle velocity. The second term on the right-hand side of (8) represents the Eulerian increment in the fluid element velocity following a particle, due to the difference in the mean particle and fluid velocities (the notation $\langle \cdot \rangle_p$ is used throughout to indicate the average computed following the particle). As shown below, this is an important difference compared to (5) in which the Eulerian increment in the fluid velocity is due to the difference in the instantaneous particle and fluid velocities. Both Langevin models (5) and (8) are used to derive transport equations for the fluid-particle covariance. The closure used for $G_{fp,ij}^*$ is the same as that employed for (5), given by (6). The closure for K_{fp} and K_{fp}^* do not enter the model expressions for the fluid-particle correlation.

2.3 Transport of the fluid-particle covariance

Using (2) for the particle equation of motion and the Lagrangian stochastic equation for the undisturbed fluid velocity at the particle position (5) or (8), transport equations can be derived for various moments of the pdf f_{fp} by the appropriate multiplication and integration of (1) over the particle and fluid velocity spaces. Using either (5) or (8), the transport of the fluid-particle covariance can be expressed as,

$$\begin{aligned} n_p m_p \left[\frac{\partial}{\partial t} + V_{p,j} \frac{\partial}{\partial x_j} \right] q_{fp} &= \underbrace{-\frac{\partial}{\partial x_j} \left[n_p m_p \langle v'_{p,j} \tilde{u}'_{f,i} v'_{p,i} \rangle_p \right]}_{\text{turbulent dispersion}} \underbrace{-n_p m_p R_{fp,ij} \frac{\partial V_{p,i}}{\partial x_j} - n_p m_p R_{ji}^* \frac{\partial U_{f,i}}{\partial x_j}}_{\text{production}} \\ &+ \underbrace{\frac{n_p m_p}{\tau_{fp}^F} [2q_f^2 - q_{fp}]}_{\text{interphase transfer}} + \underbrace{n_p m_p G_{fp,mn} R_{fp,nm}}_{\text{dissipation}}. \end{aligned} \quad (9)$$

In (9), $R_{fp,ij} = \langle \tilde{u}'_{f,i} v'_{p,j} \rangle_p$ is the fluid-particle correlation tensor where $\tilde{u}'_{f,i}$ is the i^{th} component of the fluctuating fluid velocity at the particle position, $v'_{p,j}$ is the j^{th} component of the fluctuating particle velocity, and $q_{fp} = R_{fp,kk}$. The first term on the right-hand side represents the transport of fluid-particle covariance by the particle velocity fluctuations. The second and third terms on the right-hand side are production of q_{fp} via interactions with the mean gradients of the particle and fluid velocity. The term R_{ij}^* is dependent on the form of the Langevin equation, i.e., $R_{ij}^* = R_{fp,ij}$ using (5) from Simonin *et al.* (1993) while $R_{ij}^* = R_{p,ij}$ using (8) of Minier and Peirano (2001) where $R_{p,ij} = \langle v'_{p,i} v'_{p,j} \rangle_p$ is the particle kinetic stress. The fourth term in (9) represents the effect of

interphase exchange between the dispersed and carrier phases where the notation τ_{fp}^F is introduced to define the mean particle relaxation time. The last term in (9) is the rate of dissipation.

The triple correlation term must be modeled and is closed using a gradient transport hypothesis,

$$\frac{\partial}{\partial x_j} \left[n_p m_p \langle v'_{p,j} \tilde{u}'_{f,i} v'_{p,i} \rangle_p \right] \approx - \frac{\partial}{\partial x_i} \left[n_p m_p \frac{D_{fp,ij}^t}{\sigma_{fp}} \frac{\partial q_{fp}}{\partial x_j} \right], \quad (10)$$

in which the fluid particle turbulent dispersion tensor $D_{fp,ij}^t$ and parameter σ_{fp} takes the form,

$$D_{fp,ij}^t = G_{fp,im}^{-1} R_{fp,mj} = \tau_{fp}^t R_{fp,ij}, \quad \sigma_{fp} = \frac{1}{\beta_1} \left[10 - 5.6 \frac{\eta_r}{1 + \eta_r} \right], \quad \eta_r = \frac{\tau_{fp}^t}{\tau_{fp}^F} \quad (11)$$

where σ_{fp} is calibrated to yield accurate productions of the fluid-particle covariance in equilibrium shear flow (Fevrier and Simonin 1998, Simonin 2000) and η_r represents the ratio of the eddy-particle interaction timescale to the mean particle relaxation time.

The production terms require specification of $R_{fp,ij}$ which is evaluated using the algebraic stress model (ASM) developed by Fevrier and Simonin (1998), derived by assuming equilibrium in the anisotropy tensor of the fluid-particle velocity correlation. For the form of $G_{fp,ij}$ given by (6), the ASM model is,

$$\begin{aligned} R_{fp,ij} &= \frac{\delta_{ij}}{3} q_{fp} + \frac{q_{fp}}{2q_f^2} \left[R_{f,ij} - \frac{2}{3} q_f^2 \delta_{ij} \right] \\ &+ \frac{\tau_{fp}^F}{2q_f^2} \left[q_{fp} (P_{fp,ij} + P_{ij}^*) - R_{fp,ij} (P_{fp,nn} + P_{nn}^*) \right], \end{aligned} \quad (12)$$

where $R_{f,ij}$ is the fluid Reynolds stress tensor and the terms $P_{fp,ij}$ and P_{ij}^* represent production terms due to the mean particle and fluid velocity gradients,

$$P_{fp,ij} = -R_{fp,im} \frac{\partial V_{p,j}}{\partial x_m}, \quad P_{ij}^* = -R_{mj}^* \frac{\partial U_{f,i}}{\partial x_m}, \quad (13)$$

where, as noted above in reference to (9), $R_{ij}^* = R_{fp,ij}$ using the Langevin model (5) and $R_{ij}^* = R_{p,ij}$ using (8).

For the form (6), the dissipation term in (9) takes the form,

$$G_{fp,mn} R_{fp,nm} = - \frac{q_{fp}}{\tau_{fp}^t} = -\varepsilon_{fp}. \quad (14)$$

3 Approach

3.1 LES and DPS of turbulent channel flow

The fully-developed particle-laden turbulent flow between plane, parallel walls is predicted using Large Eddy Simulation (LES) for the carrier phase and particle tracking for the dispersed phase. The fluid flow is driven by a uniform pressure gradient along the axis of the channel. The Reynolds number is $Re_\tau = 180$ where u_τ is the friction velocity and δ is the channel halfwidth. The dimensions of the channel are $4\pi\delta$ in the streamwise (x or x_1), $4\pi\delta/3$ in the spanwise (z or x_3), and 2δ in the wall-normal (y or x_2) directions. Periodic boundary conditions are applied to the dependent variables in the streamwise and spanwise dimensions and no-slip boundary conditions to the velocity at the channel walls. The subgrid stress arising from the filtering of the Navier-Stokes equations is closed using a simple fixed-coefficient eddy viscosity model.

| | | | |
|-----------------|--------|------|------|
| ρ_p/ρ_f | 527 | 2106 | 8424 |
| St | 0.1625 | 0.65 | 2.60 |
| τ_{ps}^+ | 29 | 117 | 468 |

Table 1: Particle parameters for turbulent channel flow, $Re_\tau = 180$. The particle diameter for each case is one viscous unit, $d_p^+ = 1$. The time constant in viscous units, $\tau_{ps}^+ = \tau_{ps} Re_\tau$.

The equations governing the fluid flow are solved using a fractional step method on a staggered mesh comprised of 64^3 cells. Spatial derivatives are approximated using second-order accurate central differences. The Poisson equation formulated for the pressure that is used to obtain a divergence-free velocity field is solved using fast transforms in the streamwise and spanwise direction, resulting in a series of tri-diagonal matrices that are efficiently inverted in the direction normal to the surface. The grid spacing is uniform in the x and z directions. The wall-normal mesh is clustered near the solid surfaces and stretched away from the wall using a hyperbolic tangent function. The discretized system is advanced in time using an implicit/explicit time advance (Crank-Nicholson and second-order Adams-Bashforth).

In this work, the fluid flow is not influenced by momentum exchange with the particles and the (undisturbed) fluid velocity $u_{f,i}$ required in (2) is the value interpolated to the particle position that is computed in the LES, representing the spatially-filtered (volume averaged) solution of the Navier-Stokes equations. The influence of subgrid-scale transport on particle motion is not considered, which is a reasonable assumption given the strong filtering by particle inertia of the smaller-scale, high-frequency components of the subgrid velocity for the given Stokes numbers. The neglect of subgrid transport is further justified by the low Reynolds number of the calculations and relatively weak effect of the unresolved motions on the resolved scales.

Simulations are performed for three particle Stokes numbers, $St = \tau_{ps}/(\delta/u_\tau)$, where τ_{ps} is the Stokes relaxation timescale of the particle. For all simulations the particle diameter was specified as one viscous unit and therefore the variation in the Stokes number is achieved via a variation in the density ratio, as summarized in Table 1. The particle response times are chosen so that the lightest particles ($St = 0.1625$) follow reasonably well the turbulent fluctuations in the carrier phase, while for the largest $St = 2.60$ the particles are largely unaffected by the carrier flow.

Properties of the dispersed phase are obtained by following the trajectories of 1×10^5 particles, corresponding to an average number density of 950 particles per unit volume, equivalent to a dispersed-phase volume fraction of 8.5×10^{-5} . The particle equation of motion (2) is integrated in time using second-order Adams-Bashforth. Third-order Lagrange polynomials are used to interpolate the fluid velocity to the particle position. Particle displacements are also integrated using the second-order Adams-Bashforth method. For particles that move out of the channel in the streamwise or spanwise directions, periodic boundary conditions are used to reintroduce them into the computational domain.

A particle is assumed to contact the smooth channel walls when its center is one radius from the wall, and elastic collisions are enacted for wall contact events. Some of the simulations include the effects of inter-particle collisions. Particle-particle collisions are detected using an algorithm similar to that outlined by Sundaram and Collins (1997). To avoid the full quadratic expense of naive collision detection by checking the entire ensemble of collision partners for each particle, the physical domain is divided into a three-dimensional array of cells. The list of possible collision partners for a given particle is then restricted to the smaller subvolumes. Only binary collisions are considered, and all particle-particle collisions are perfectly elastic. The reader is referred to Vance and Squires (2002) for further details on the collision algorithm employed for the current simulations.

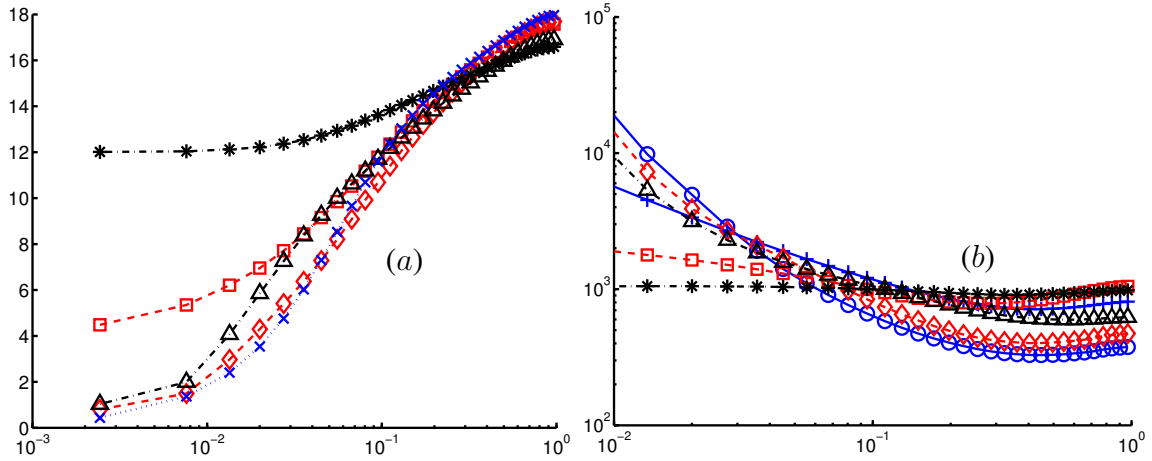


Figure 1: (a) streamwise mean velocity for $St = 0.65$ and $St = 2.60$. (b) number density. $St = 0.1625$: $\circ-\circ$ without collisions; $+--+$ with collisions; $St = 0.65$: $\diamond-\diamond$ without collisions; $\square--\square$ with collisions; $St = 2.60$: $\triangle--\triangle$ without collisions; $*--*$ with collisions; $\times\cdots\cdots\times$ fluid.

3.2 Procedure for *in medio* tests

The fluid-particle covariance transport equation (9) is solved for fully developed particle-laden channel flow using an *in medio* approach in which some terms are evaluated using the LES/DPS database while models are employed for other terms. In particular, LES results for the mean fluid velocity gradient, mean particle velocity gradient, fluid kinetic energy, and particle kinetic energy are used to evaluate the terms where those quantities appear in (9). The components of the fluid-particle velocity correlation tensor are evaluated using the ASM model (12). The triple correlation term is modeled, in addition to the dissipation rate, ε_{fp} , via the specification of the eddy-particle interaction time (7).

An iterative scheme is used to solve the coupled system represented by (9) and (12). The eddy-particle interaction time is computed using (7), and the fluid-particle diffusion tensor, $D_{fp,ij}^t$, is calculated using (11). The remaining quantities are held fixed to their values from the LES database. The iterations of the system are continued to convergence, defined as a reduction in the residual by seven orders of magnitude.

4 Results

4.1 Dispersed-phase statistics

Shown in Figure 1 are profiles of the streamwise mean particle velocity in the left-hand frame and mean number density in the right-hand frame. Comparison of the profiles of the mean velocity for a given Stokes number in Figure 1a shows that there is an increasingly strong effect of inter-particle collisions with increases in Stokes number. In the flows without particle-particle collisions, Figure 1a shows that the mean streamwise particle velocity are closer to the mean fluid velocity with particles leading the fluid flow near the wall and slightly lagging in the channel core. The effect of inter-particle collisions increases transport across the channel, one consequence being that the mean flow becomes more uniform. The streamwise mean velocity is largest, for example, in the near-wall region for $St = 2.60$.

The change in the number density with Stokes number and inter-particle collisions is illustrated in Figure 1b. The flows without inter-particle collisions exhibit an accumulation of particles in the near-wall region, a well-known effect observed in many previous computations that do not include inter-particle collisions. Changes in wall-normal (“radial”) transport across the channel induced by inter-particle collisions leads to a more uniform number density profile, as shown in Figure 1b. For

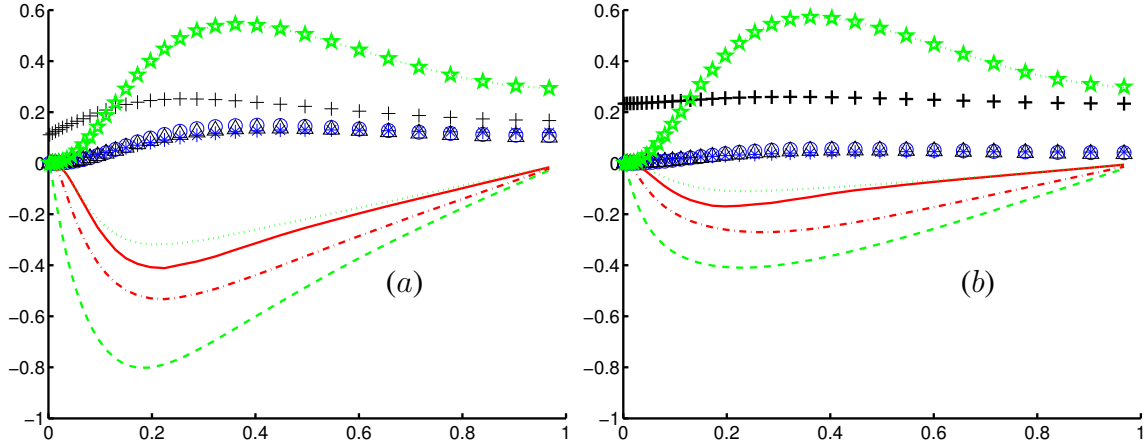


Figure 2: Wall-normal components of the fluid-particle ($R_{fp,22}$, $R_{fp,21}$), particle ($R_{p,22}$) and fluid ($R_{f,22}$) velocity correlations. (a) $St = 0.65$; (b) $St = 2.60$. $\star R_{f,22}$. Without inter-particle collisions: $\circ R_{fp,22}$; $\ast R_{p,22}$; — $R_{fp,21}$; - - - $R_{p,21}$. With inter-particle collisions: $\triangle R_{fp,22}$; $+$ $R_{p,22}$; $R_{fp,21}$; - - - $R_{p,21}$;

the smallest Stokes number $St = 0.1625$, the number density peaks near the wall, as observed in the profile without inter-particle collisions, though is less pronounced compared to the non-colliding case. Increases in the Stokes number lessen the non-uniformity in the distribution and Figure 1b shows that the number density profile is nearly uniform for $St = 2.60$.

Shown in Figure 2 are profiles of the wall-normal components of the particle kinetic stress $R_{p,22}$, fluid stress $R_{f,22}$, and two components of the fluid-particle correlation tensor, $R_{fp,22}$ and $R_{fp,21}$. Figure 2a is from computations with and without colliding particles for $St = 0.65$. Figure 2b shows the same statistics for $St = 2.60$. For the flows without inter-particle collisions both figures show that the wall-normal components of the particle kinetic stress and fluid-particle correlation are nearly equal, i.e., $R_{p,22} \approx R_{fp,22}$. This equivalence in the flows without collisions reflects the fact that the particle velocity fluctuations in the wall-normal direction (and spanwise direction, not shown) are controlled by the drag force and in local equilibrium with turbulent fluid flow (e.g., see Hinze 1975). In addition, comparison of the profiles of $R_{p,22}$ for $St = 0.65$ and $St = 2.60$ in the simulations with non-colliding particles shows that the wall-normal particle velocity fluctuations are damped with increases in the Stokes number. This is further consistent with the equivalence between $R_{p,22}$ and $R_{fp,22}$ and the control of the wall-normal (and spanwise) velocity fluctuations by the drag in flows without inter-particle collisions.

The effect of inter-particle collisions is to re-distribute the kinetic energy of the particle fluctuations with one consequence being an increase in the wall-normal kinetic stress, $R_{p,22}$, compared to the simulations that do not include particle-particle collisions. In addition, comparison of the levels in $R_{p,22}$ for $St = 2.60$ in Figure 2b to the same curve for $St = 0.65$ in Figure 2a (given by the $+$ symbols in each frame) shows that the wall-normal particle fluctuating velocities are larger for the larger Stokes number close to the wall. In addition, for both Stokes numbers the wall-normal particle fluctuating velocities are larger than the corresponding value for the fluid in the region from the wall to about $y/\delta = 0.1$. Both frames of Figure 2 show that the equilibrium between the particle fluctuations and fluid-particle correlation that is observed in the flows without inter-particle collisions is disrupted, i.e., $R_{p,22}$ and $R_{fp,22}$ are no longer equivalent. Figure 2 also shows that for both Stokes numbers the fluid-particle correlation $R_{fp,21}$ exhibits only small changes due to the effect of inter-particle collisions.

4.2 Model evaluations using the *in medio* approach

Figure 3 shows the balance of the terms in the fluid-particle velocity covariance transport equation (9). The balance obtained from the LES database is shown using symbols, model predictions using (5) are shown by the lines. The balance of the terms in the exact equation for q_{fp} are evaluated from,

$$\begin{aligned}
 n_p m_p \left[\frac{\partial}{\partial t} + V_{p,j} \frac{\partial}{\partial x_j} \right] q_{fp} = & \underbrace{-\frac{\partial}{\partial x_j} \left[n_p m_p \langle v'_{p,j} \tilde{u}'_{f,i} v'_{p,i} \rangle_p \right]}_{\text{turbulent dispersion}} \underbrace{-n_p m_p R_{fp,ij} \frac{\partial V_{p,i}}{\partial x_j} - n_p m_p R_{fp,ji} \frac{\partial U_{f,i}}{\partial x_j}}_{\text{production}} \\
 & + \underbrace{n_p m_p \left\langle \frac{dv_{p,i}}{dt} \tilde{u}'_{f,i} \right\rangle_p}_{\text{interphase transfer}} + \underbrace{\left\langle \left[\frac{d\tilde{u}_{f,i}}{dt} - (v_{p,j} - \tilde{u}_{f,j}) \frac{\partial \tilde{U}_{f,i}}{\partial x_j} \right] v'_{p,i} \right\rangle_p}_{\text{dissipation}}. \quad (15)
 \end{aligned}$$

The general features of the balance of the exact terms from (15) for all Stokes numbers and with or without particle-particle collisions show that the interphase transfer term, accounting for production of q_{fp} by the drag force, is comparable to the production term arising from interactions with the mean shear of the particle and fluid velocities. For $St = 2.60$, for example, Figure 3e shows that the interphase transfer term and mean shear production are comparable in the flow that includes inter-particle collisions. The left-hand frames in Figure 3 also show that the balances from the simulations including colliding particles indicate that the magnitude of the shear production is smaller as compared to the flows without inter-particle collisions (corresponding right-hand frames in Figure 3). This feature is in turn consistent with smaller gradients in the particle mean velocity profile in the flows including inter-particle collisions (c.f., Figure 1a). Finally, the turbulent dispersion term is significant below $y/\delta \approx 0.2$, essentially zero in the outer region of the flow.

The q_{fp} balances resulting from the *in medio* tests shown in Figure 3 are those from the models developed using the Lagrangian stochastic equation (5) proposed by Simonin *et al.* (1993). Overall, there is a reasonable accounting of the behavior of the terms governing the transport of q_{fp} . Outside of $y/\delta \approx 0.2$, the models accurately account for the evolution of the terms in the q_{fp} balance over the entire range of Stokes numbers and in the flows with and without inter-particle collisions. As the figure shows, the greatest discrepancy between the modeling and LES results occurs in the turbulent dispersion term which is under-predicted compared to the simulation database using the relation (10).

The mean-shear production terms in Figure 3 are relatively accurate for both flow types (with and without colliding particles) for $St = 0.1625$ and $St = 0.65$ with the model predictions slightly higher than the peak shear production obtained from the simulation database (c.f., Fig. 3a-d). For $St = 2.60$ there are larger differences between the model prediction of the shear-production term and the LES database (c.f., Fig. 3e,f). Because the mean velocity gradients used in the *in medio* evaluations are taken from the LES database, the errors in the shear production reflect differences arising from errors in other terms (e.g., the turbulent dispersion) as well as from errors in the prediction of $R_{fp,12}$, which is the component of the fluid-particle correlation tensor multiplying the mean velocity gradients in the production for fully-developed channel flow. The contribution of interphase transfer to the q_{fp} balance is accurately predicted for the larger Stokes numbers $St = 0.65$ and $St = 2.60$. For the smallest Stokes number both Figure 3a and Figure 3b show that the model predicts a peak in the interphase transfer that is higher than the LES result and nearer the wall. The dissipation rate is predicted reasonably accurately for each Stokes number and in the flows with and without inter-particle collisions. For $St = 0.1625$, the model predictions of the dissipation rate are above the LES results in the region $y/\delta \approx 0.1$, consistent with the under-prediction of the turbulent dispersion term in this region (c.f., Fig. 3a,b). At the largest Stokes number $St = 2.60$ the peak in the dissipation rate yielded from the *in medio* tests of the modeling is below the LES result for both flow types.

Figure 4 shows the comparison between the *in medio* predictions of q_{fp} and the LES results, again using the models based on the Lagrangian stochastic equation of Simonin *et al.* (1993). The

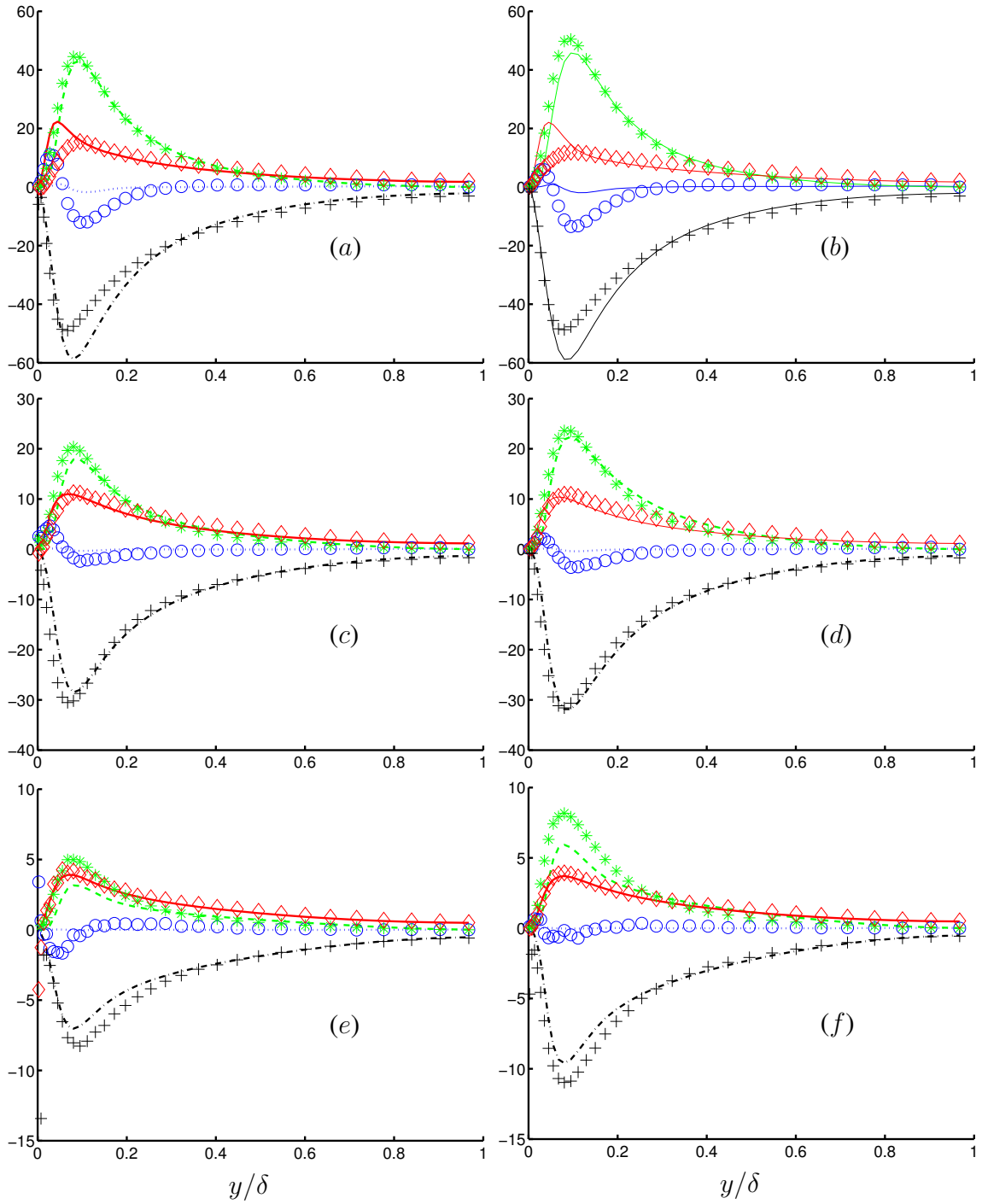


Figure 3: Balance of the q_{fp} transport equation. Symbols are the exact terms from the LES database, lines are the model predictions using (5). Left frames from simulations with inter-particle collisions, right frames from simulations without inter-particle collisions. $St = 0.1625$: (a) and (b); $St = 0.65$: (c) and (d); $St = 2.60$: (e) and (f). ---- * production; ——— \diamond interphase transfer; \circ turbulent dispersion; -.-.- + dissipation.

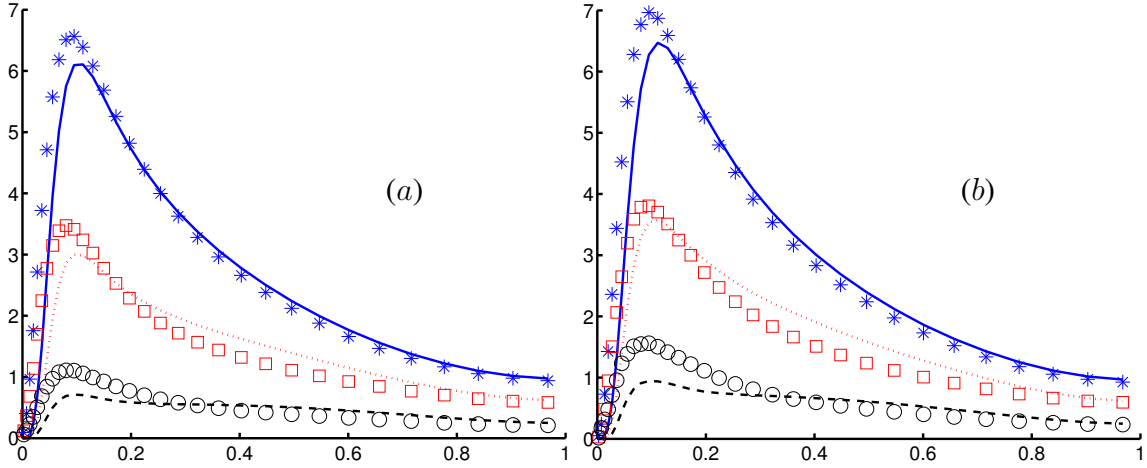


Figure 4: Measured and predicted fluid-particle covariance, q_{fp} . (a) with-collisions; (b) without-collisions. Symbols are the LES results, lines are the model predictions using (5). —, * $St = 0.1625$; , \square $St = 0.65$; ----, \triangle $St = 2.60$.

overall agreement between the model prediction and LES results is reasonable for the smaller Stokes numbers, $St = 0.1625$ and $St = 0.65$, both with and without the influence of inter-particle collisions. As observed earlier for the q_{fp} balances, for $y/\delta > 0.2$ there is good (for $St = 0.1625$) or fair (for $St = 0.65$) agreement between the models and LES results. The peak values in q_{fp} for the smaller Stokes numbers are slightly lower than the LES. For the larger Stokes number $St = 0.65$, Figure 4a,b show that the model predictions again exhibit a reasonable agreement with the LES results, though the under-prediction of the peak value is more apparent.

The assessment of the predictions of the fluid-particle correlations summarized above were based on the use of the Lagrangian stochastic equation (5). Shown in Figure 5 is a comparison of the elements of the fluid-particle correlation tensor $R_{fp,ij}$ from the *in medio* evaluations based on (5) proposed by Simonin *et al.* (1993) (left-hand frames of the figure) to those from *in medio* evaluations based on (8) and proposed by Minier and Peirano (2001) (right-hand frames of the figure). The comparisons in Figure 5 show the results obtained for $St = 0.65$, both with and without the effect of inter-particle collisions.

Figure 5a,b show the streamwise component, $R_{fp,11}$. While the model predictions arising from the use of the Lagrangian stochastic equation (5) yield a reasonable accounting of this component for flows with and without inter-particle collisions, the model predictions in Figure 5b based on (8) are not accurate in the flow with colliding particles. An analogous behavior is noted in Figure 5d in which use of the Lagrangian stochastic equation (8) leads to large over-predictions of $R_{fp,12}$ in the flow that includes inter-particle collisions.

As noted in the presentation of the models, the differences in the formulations obtained using (5) and (8) is the term R_{ij}^* in (9) and (12). Using (8) from Minier and Peirano (2001), $R_{ij}^* = R_{p,ij}$ whereas using (5) from Simonin *et al.* (1993), $R_{ij}^* = R_{fp,ij}$. In the fully-developed channel flow this reduces to $R_{p,21}$ or $R_{fp,21}$ in (9) and $R_{p,22}$ or $R_{fp,22}$ in (12). In the flow without inter-particle collisions, Figure 2 showed that $R_{p,22} \approx R_{fp,22}$ and that there are not large differences between $R_{p,21}$ and $R_{fp,21}$. Consequently, the model predictions in Figure 5 based on (8) proposed by Minier and Peirano (2001) yields similar accuracy as the predictions obtained from (5).

As Figure 2 also illustrates, however, there are large differences between the particle kinetic stress $R_{p,22}$ and fluid-particle correlation $R_{fp,22}$ in flows with inter-particle collisions. The wall-normal particle kinetic stress $R_{p,22}$ can be much larger than $R_{fp,22}$ because of the redistribution of the particulate phase kinetic energy by collisions. In the fluid-particle correlation model based on (8), $R_{fp,12}$ is

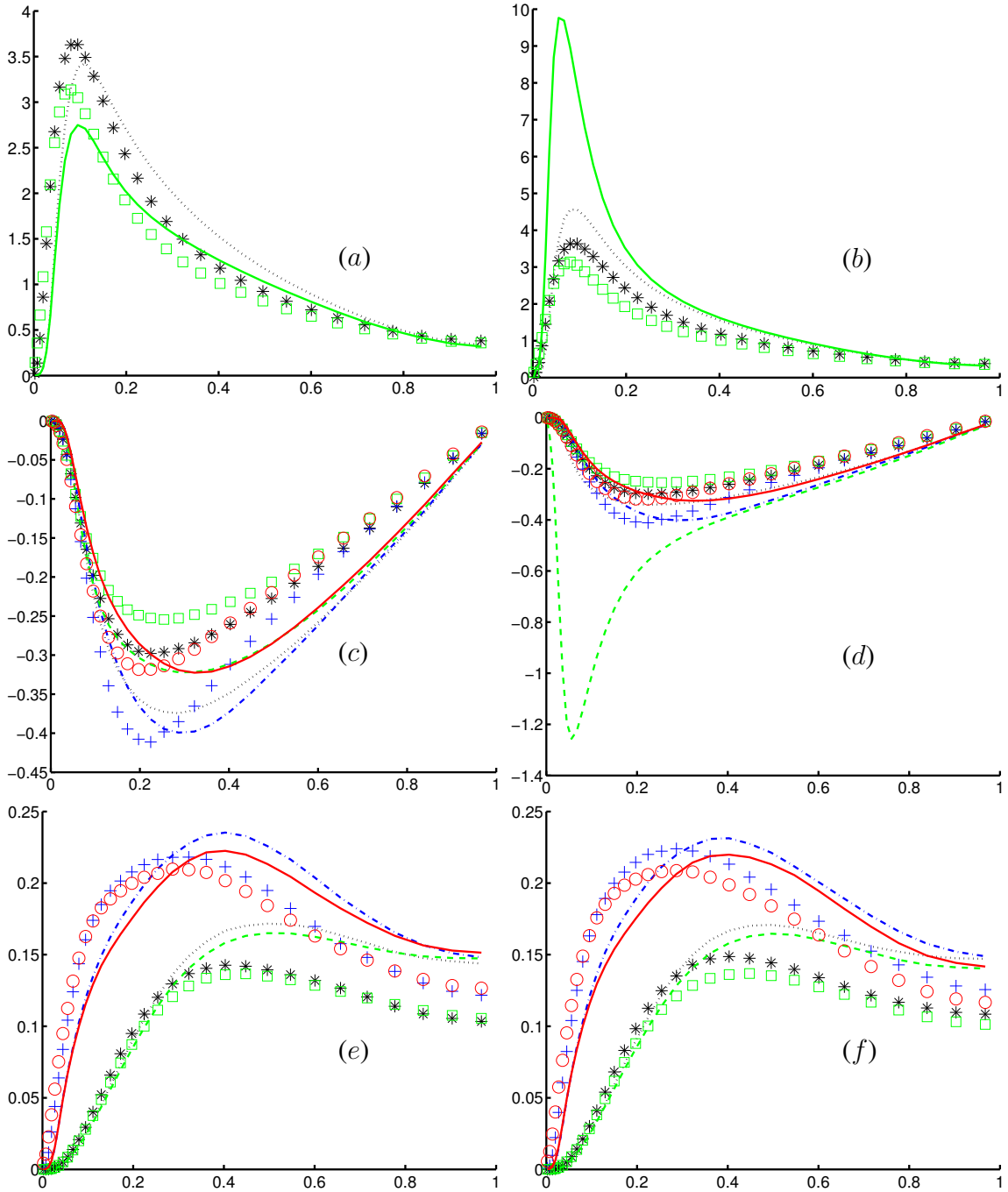


Figure 5: Measured and predicted fluid-particle correlation, $R_{fp,ij}$, $St = 0.65$. Symbols are LES results, lines are model predictions. Left frames are obtained using (5). Right frames are obtained using (8). (a) and (b) $R_{fp,11}$: *, * without collisions; —, □ with collisions; (c) and (d) $R_{fp,12}$: * without collisions; ---- □ with collisions. $R_{fp,21}$: —+ without collisions; —, ○ with collisions; (e) and (f) $R_{fp,22}$: * without collisions. ---- □ with collisions; $R_{fp,33}$: —+ without collisions; —, ○ with collisions;

amplified since this component depends on $R_{p,22}$ using the approach of Minier and Peirano (2001). The streamwise component $R_{fp,11}$ depends on $R_{fp,12}$ via (12) and the over-prediction in $R_{fp,12}$ subsequently leads to a large over-prediction in $R_{fp,11}$. Figure 5e,f shows that the predictions of the diagonal components, $R_{fp,22}$ and $R_{fp,33}$, are very similar for the two models for both flow types. Based on the over-prediction of the streamwise component in Figure 5b, it is apparent that using the Lagrangian stochastic model (8), the trace of the tensor, q_{fp} , would also be over-predicted.

These differences in the model predictions arise because of the different formulations (5) and (8) and are important because they change the form of the shear-production term. The difference in the shear-production term between the two models is related to the turbulent relative velocity between the phases and is increased when inter-particle collisions take place, in turn highlighting the differences in the model predictions and LES results in Figure 5b,d arising from the use of (8).

5 Summary

The database from LES/DPS of particle-laden turbulent channel flow was used to assess models for the fluid-particle velocity correlation. The Stokes number range was sufficiently broad to explore regimes in which the particles track the carrier phase fluid velocity reasonably well to regimes in which the particles are unresponsive to the bulk of the turbulent eddies. While the dispersed-phase volume fraction was relatively low, the LES/DPS show a significant effect of inter-particle collisions on dispersed phase transport for the higher Stokes numbers.

The model predictions for the fluid-particle velocity correlation based on the Lagrangian stochastic equation proposed by Simonin *et al.* (1993) leads to reasonable predictions of the fluid-particle correlation tensor. In contrast, the models based on the approach of Minier and Peirano (2001) lead to comparable accuracy only in the flows that do not include the effects of inter-particle collisions. Disrupting the equilibrium between the particle fluctuating velocity and fluid-particle correlation, as occurs in the flows with inter-particle collisions, lead to over-predictions of some components of $R_{fp,ij}$.

While obtaining encouraging predictions of the fluid-particle correlation based on (5) for the parameter ranges considered, the simple form for the eddy-particle interaction timescale is probably not sufficient for more general settings, especially when there are strong effects of crossing trajectories. In the present investigations, the greatest discrepancies in prediction of the fluid-particle correlations using (5) are noted for the largest Stokes number, which corresponds to the particle relaxation timescale with the largest slip between the phases and providing some evidence of the need to improve the timescale prescription describing the fluid turbulence viewed by the particles.

Finally, the *in medio* procedure provides more insight into the performance of a model than typical *a priori* tests. The *in medio* procedure is a valuable tool for assessing statistical models and is not restricted to an LES/DPS database as was used in the current investigations. Sufficiently detailed experimental measurements could also be used to supply quantities such as the mean velocity gradients and fluid kinetic energy, for example. Such studies in more complex flows that include more effects than in this work would be valuable.

References

- [1] Fevrier, P. and Simonin, O., "Constitutive relations for fluid-particle velocity correlations in gas-solid turbulent flows", *3rd Intl. Conf. on Multiphase Flows*, Lyon, France, June 8-12, 1998.
- [2] Hanjalic, K., "Advanced turbulence closure models: a view of current status and future prospects", *Int. J. Heat and Fluid Flow*, **15**, pp. 178-203, 1994.

- [3] Hinze, J.O., *Turbulence*, New York, Mc Graw-Hill, 1975.
- [4] Minier, J.P. and Peirano, E., “The PDF approach to turbulent polydispersed two-phase flows”, *Physics Reports*, **352**, pp. 1-214, 2001.
- [5] Parneix, S., Laurence, D. and Durbin, P.D., “A procedure for using DNS databases”, *J. Fluids Eng.*, **120**, pp. 40-47, 1998.
- [6] Schiller, L. and Nauman, A., “A Drag Coefficient Correlation:”, *V.D.I. Zeitung*, **77**, pp. 318-320, 1935.
- [7] Simonin, O., Deutsch, E. and Minier, J.P., “Eulerian prediction of Fluid-Particle Correlated Motion in Turbulent Two-Phase Flows”, *Applied Scientific Research*, **51**, pp. 275-283, 1993.
- [8] Simonin, O., “Statistical and continuum modelling of turbulent reactive particulate flows. Part 1: theoretical derivation of dispersed Eulerian modelling from probability density function kinetic equation”, in *Theoretical and Experimental Modeling of Particulate Flows, Lecture Series 2000-06*, von Karman Institute for Fluid Dynamics, Rhode Saint Genése (Belgium), 2000.
- [9] Sommerfeld, M., “Theoretical and experimental modeling of particulate flow: overview and fundamentals”, *VKI for fluid dynamics, Lecture Series 2000–06*, 2000.
- [10] Sundaram, S. and Collins, L.R., “Collision statistics in an isotropic particle-laden turbulent suspension. Part 1. Direct numerical simulations”, *J. Fluid Mech.*, **335**, pp. 75-109, 1997.
- [11] Vance, M.W. and Squires, K.D., 2002, An approach to parallel computing in an Eulerian-Lagrangian two-phase flow model, *FEDSM 2002-31225*.